ACS APPLIED MATERIALS & INTERFACES

Research Article

www.acsami.org

Logic Nanoparticle Beacon Triggered by the Binding-Induced Effect of Multiple Inputs

Jing Yang,*[,†] Chen Dong,[‡,§] Yafei Dong,[‡] Shi Liu,[†] Linqiang Pan,*[,∥] and Cheng Zhang*[,§]

[†]School of Control and Computer Engineering, North China Electric Power University, Beijing 102206, China

[‡]College of Life Science, Shannxi Normal University, Xi'an 710062, China

[§]Institute of Software, School of Electronics Engineering and Computer Science, Key Laboratory of High Confidence Software Technologies of Ministry of Education, Peking University, Beijing 100871, China

[∥]Key Laboratory of Image Information Processing and Intelligent Control, School of Automation, Huazhong University of Science and Technology, Wuhan 430074, China

Supporting Information

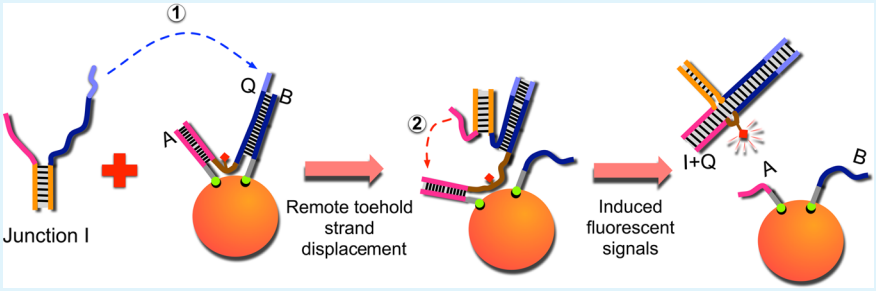

ABSTRACT: Recently, the toehold-mediated DNA strand displacement reaction has been widely used in detecting molecular signals. However, traditional strand displacement, without cooperative signaling among DNA inputs, is insufficient for the design of more complicated nanodevices. In this work, a logic computing system is established using the cooperative "binding-induced" mechanism, based on the AuNP-based beacons, in which five kinds of multiple-input logic gates have been constructed. This system can recognize DNA and protein streptavidin simultaneously. Finally, the manipulations of the logic system are also demonstrated by controlling programmed conjugate DNA/AuNP clusters. This study provides the possibility of detecting multiple input signals and designing complex nanodevices that can be potentially applied to the detection of multiple molecular targets and the construction of large-scale DNA-based computation.

KEYWORDS: *fluorescent beacon, binding-induced strand displacement, DNA self-assembly, gold nanoparticle, logical computing*

INTRODUCTION

Nucleic acids (i.e., DNA and RNA) are attractive materials for many researchers in interdisciplinary fields such as nanotechnology, chemistry, and medicine because of their specificity recognition and signal diversity via Watson−Crick base pairing. Recently, DNA computing has become an emerging field focusing on biological circuits[1−5] and molecular detection.[6−9]

In previous studies, molecular logic detecting systems were established not only to detect DNA molecules but also to recognize many other materials, using complicated elements of deoxyribozymes,[10,11] G-quadruplex DNA,[12,13] and AuNP-based beacons.[14−18] In particular, the toehold-mediated DNA strand displacement reaction has been widely used in detecting molecular signals for its characteristic highly specific recognition and cascading circuit. In practice, a variety of logic computing devices have been established, such as element gates,[19,20] neural networks,[21] and computing circuits,[22,23] on the basis of this principle. However, most of those studies implemented traditional strand displacement, in which the input DNA signals just directly triggered their targets, without cooperative signaling among them.[24−26] Therefore, it is insufficient to meet the requirements for the design of more complicated and delicate computing systems. In our study, to address this problem, we proposed a "binding-induced" method, with which one combinational DNA input signal can be "created" by cooperatively binding other component DNA strands.[27,28] Subsequently, the newly generated inputs can trigger downstream strand displacements accordingly.

On the other hand, the AuNP-based beacons, possessing several advantages such as strongly quenching effects and sensitive sequence specificity,[29−33] have attracted widespread attention in recent years. Therefore, it is of particular interest to use the binding-induced method with AuNP-based beasons, to detect complex DNA signals. In addition, logically detecting multiple kinds of input signals at the same time remains a

Received: June 14, 2014
Accepted: August 4, 2014
Published: August 4, 2014

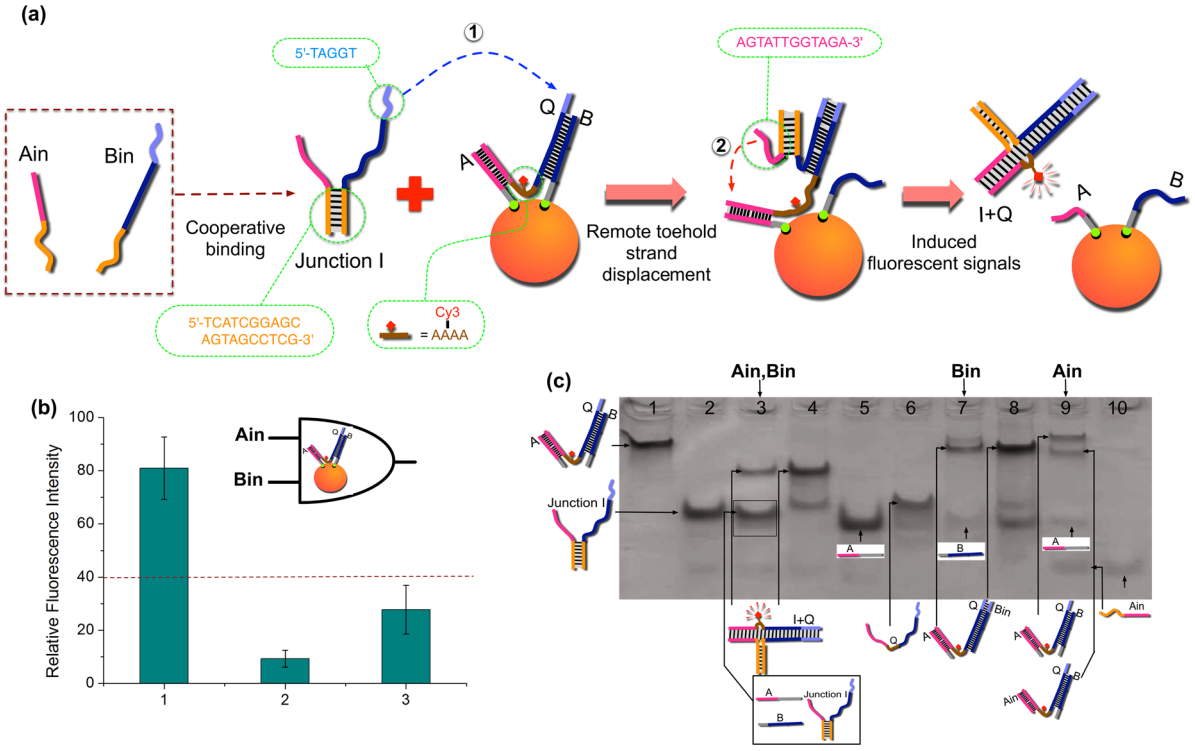

Figure 1. Two-input "AND" logic gate G1. (a) Illustration of the operational design of the two-input "AND" gate. (b) Fluorescence results. Error bars represent one standard deviation from triplicate analysis. The threshold is set at half of the highest signal value. (c) PAGE gel (12%) analysis of the gate. The concentration for each input DNA is 6 μM, while the concentration for gate ABQ is 3 μM. Lanes 1, 2, 4, and 8 correspond to different assembly products: ABQ, junction I, (**I+Q**), and nanostructure AQBin, respectively. Lanes 5, 6, and 10 correspond to single-stranded DNAs A, B, and Ain, respectively. Lanes 3, 7, and 9 correspond to the computation results of the two-input logic gate.

challenge, greatly hindering the utilization of DNA detecting systems in biomedical areas.

In this work, a logic computing system is established to verify the binding-induced mechanism, using the AuNP-based beacons, in which several kinds of multiple-input logic gates have been constructed. With versatile targeting ability to detect multiple kinds of signals, the system can recognize DNA and protein streptavidin (SA) simultaneously. Interestingly, we observed that, with the increase in the structural complexity of the combinational DNA inputs, the increments of fluorescence intensity can be significantly inhibited. Finally, the manipulations of the multiple-input logic system are also demonstrated by controlling programmed conjugate DNA/AuNP clusters.

EXPERIMENTAL METHODS

Preparation of AuNP-Based Beacons. Thiolated DNA strands A and B were mixed with strand Q or both strands Q′ and P to a final concentration of 12 μM in 0.5× TBE buffer. The mixture was incubated under the reaction condition at 37 °C for 2 h. Subsequently, the annealing products (nanostructure ABQ or ABQ′P) were incubated with a specific ratio of AuNPs (10:1) in 0.5× TBE buffer and a final concentration of 50 mM NaCl for 4−6 h at room temperature. Finally, a 2% agarose gel was used to separate the AuNPs with different discrete DNA bands for 1.5 h. The target bands of the DNA/AuNP conjugate were run in a glass fiber filter membrane assisted by a dialysis membrane (molecular weight cutoff of 14000). The conjugates were then collected in test tubes. Each sample was quantified by its optical absorbance at 520 nm and adjusted to absorption $A \approx 0.9$ and then preserved at 4 °C.

Preparation of Junction Structures. The DNA molecules were dissolved in water for hybridization. Junctions **I**−**III** were formed by mixing various equimolar DNA strands to a final concentration of 3 μM in 1× TAE/Mg^{2+} buffer [0.04 M Tris acetate, 1 mM EDTA, and 12.5 mM Mg acetate (pH 8.3)] or 0.5× TBE buffer [89 mM Tris, 89 mM boric acid, and 2 mM EDTA (pH 8.0)]. The mixture was heated at 94 °C for 5 min, slowly cooled to room temperature, and preserved at 4 °C.

Displacement Reaction of Input Junction Structures. Logic gates (consisting of the AuNP-based beacons) were displaced in 0.5× TBE buffer, at a final concentration of 0.6 μM. Input junction structures (0.6 μM) were added to a solution containing DNA gates and reacted for more than 2 h at room temperature. Next, the displaced products were stored at 4 °C for PAGE or fluorescence detection.

Fluorescence Experiments. Each logic gate sample was diluted to a final volume of 200 μL for detection, with a 120 pmol gate strand and a 120 pmol input structure. After input strands had been added to react for 2 h or other specific time intervals, the results were obtained using a spectrophotometer (Hitachi F-2700) with excitation at 550 nm and emission at 564 nm. DNA displacements were conducted at room temperature in 0.5× TBE buffer with a final NaCl concentration of 50 mM. The relative fluorescence intensity $\Delta I = (F - F_0)/F_0$, where F_0 is the background fluorescence intensity before incubation and F is the fluorescence intensity after incubation for 20 h. Accordingly, the fluorescence intensities of inputs (0,0) and (0,0,0) are zero, which have no meaning for comparisons and are not shown in Figures 1b−4b.

Native Polyacrylamide Gel Electrophoresis (PAGE). The DNA solutions mixed with 6× loading buffer (Takara) were analyzed in a 12% native polyacrylamide gel. Electrophoresis was conducted in 0.5× TBE buffer at a constant voltage of 100 V for 2 h.

TEM Analysis. Purified DNA/AuNP conjugates were freshly isolated. A 3−6 μL droplet of the sample was deposited on TEM grids (400 mesh, Ted Pella), and the excess solution was removed by using a piece of filter paper. After this, the grid was washed with Milli-Q water one to three times. TEM images were obtained by a Hitachi H-7650 transmission electron microscope.

Streptavidin Experiments. To assay for streptavidin, a sample was incubated in a 200 μL reaction mixture containing 2.2 nM AuNP-based beacon B2 (OD = 2.9×10^{-3} μM), 50 nM input DNA strands, 38.4 nM streptavidin, and 0.5× TBE buffer with a final NaCl concentration of 50 mM. The AuNP-based beacon consisted of strands A, B, P, and Q′. The

dx.doi.org/10.1021/am5036994 | ACS Appl. Mater. Interfaces 2014, 6, 14486−14492

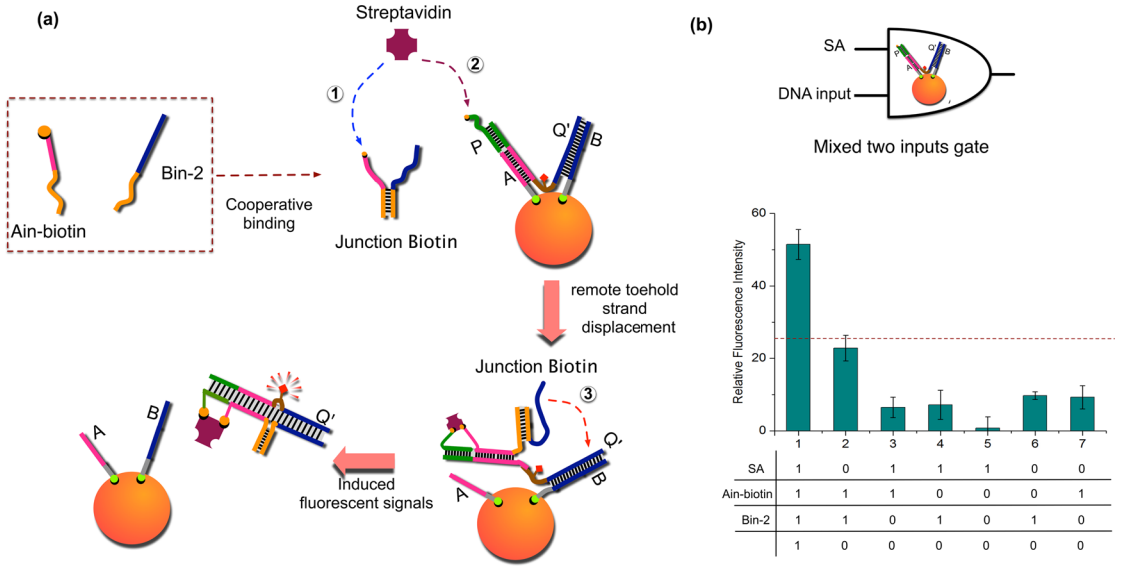

Figure 2. Mixed-input "AND" logic gate G2. (a) Illustration of the operational design. (b) Fluorescence results at 564 nm. The threshold is set at half the highest signal value.

results of the mixture were detected using a spectrophotometer with excitation at 550 nm and emission at 564 nm at a 3 h interval. The relative fluorescence intensity as a function of the logarithmic value of streptavidin concentrations is shown in Figure S5 of the Supporting Information.

RESULTS AND DISCUSSION

To implement binding-induced triggering, the AuNP-based beacon (B1) was constructed as a report gate, consisting of strands A (18 nucleotides), B (26 nucleotides), and Q (47 nucleotides) and 15 nm AuNPs (Figure 1d) (see Table S1 of the Supporting Information). As in our previous work,[34] a nanostructure ABQ was first formed by hybridizing strands A, B, with Q (modified with the fluorophore Cy3 in the middle). Then, the ABQ complex molecules were attached to 15 nm AuNPs via thiol groups of strands A and B to yield a fluorescent nanoparticle beacon. When the input strands were cooperatively assembled into junction structures, strand Q could be effectively displaced and released from the surface of AuNPs, thus leading to an increment of fluorescence intensity.

Figure 1a depicts the operations of the two-input "AND" logic gate (G1). In this section, strands Ain (22 nucleotides) and Bin (35 nucleotides) are used as the two input strands, which can form a cooperative binding structure via the complementary sequence regions. At first, when both strands Ain and Bin were added, combinational DNA junction **I** was generated and first recognized the toehold region of strand Bin, triggering the release of strand B through the displacement reaction (Figure 1a, ①). Subsequently, strand A was also displaced by strand Ain, via a mechanism of remote strand displacement.[35] Thus, the release of strand Q from AuNPs was stimulated by the binding-induced step (Figure 1a, ②), and a significant fluorescent signal was observed (Figure 1b, lane 1). However, when no strand or only one strand (Ain or Bin) was input, the fluorescence values remained low (Figure 1b, lanes 2 and 3).

The result for logic gate G1 was also confirmed by PAGE (Figure 1c). As expected, only when two input strands Ain and Bin were present simultaneously could strand Q be totally released in lane 3, subsequently leading to the formation of the byproduct of structure **I+Q**. However, with the addition of strand Bin, strand Q could be only partially displaced and assembled into a new nanostructure AQBin, and there was no product band of structure **I+Q** (lane 7). Similarly, upon addition of only strand Ain, most products of nanostructure ABQ in lane 9 were intact, although with a small ratio of displacing products (the weak band indicated by a red arrow). The possible reason may be attributed to a high concentration of strand Ain (6 μM), resulting in the partial release of strand Q.

To broaden the molecular detecting scope, we further designed another mixed-input "AND" logic gate G2, by introducing streptavidin as one of the inputs instead of just using DNA materials. Unlike initial beacon B1, without any exposed toehold region, the DNA scaffolds on AuNPs (B2) were composed of four DNA strands, P (3′-end-labeled with biotin, 37 nucleotides), Q′ (53 nucleotides), A, and B (Figure 2a). In the case of adding DNA inputs, Ain-biotin (3′-end-labeled with biotin, 52 nucleotides) and Bin-2 (28 nucleotides), they can bind with each other to form junction biotin. Next, in the presence of SA (38.4 nM), through a connection of SA and biotin, fluorescence strand Q′ can be released via remote strand displacement. As a consequence, a significant fluorescence signal was generated (Figure 2b, lane 1). As a control, in the absence of SA, even though DNA inputs Ain-biotin and Bin-2 were present, the displacement of output Q′ was difficult to conduct, and no significant fluorescence signal was observed (Figure 2b, lane 2). The measured fluorescence intensities were proportional to the concentration of streptavidin in the range of 0.1−60 nM (Figure S5 of the Supporting Information), which provided a quantitative measure of the protein concentration. Furthermore, several control experiments were implemented by adding fewer than three inputs. When any one or two inputs (SA, Ain-biotin, and Bin-2) were added, there was no significant fluorescence signal (Figure 2b, lanes 5−7 and 2−4). These results suggest that this mixed-input gate still had a strong specific detecting ability when treated with multiple kinds of molecular inputs.

To further verify feasible manipulations of this strategy, three-input "AND" logic gate G3 was established by using three strands, Ain-2 (24 nucleotides), Bin (35 nucleotides), and AB (20 nucleotides). Notably, three strands can be cooperatively associated via the binding domain to form four-way junction **II**.

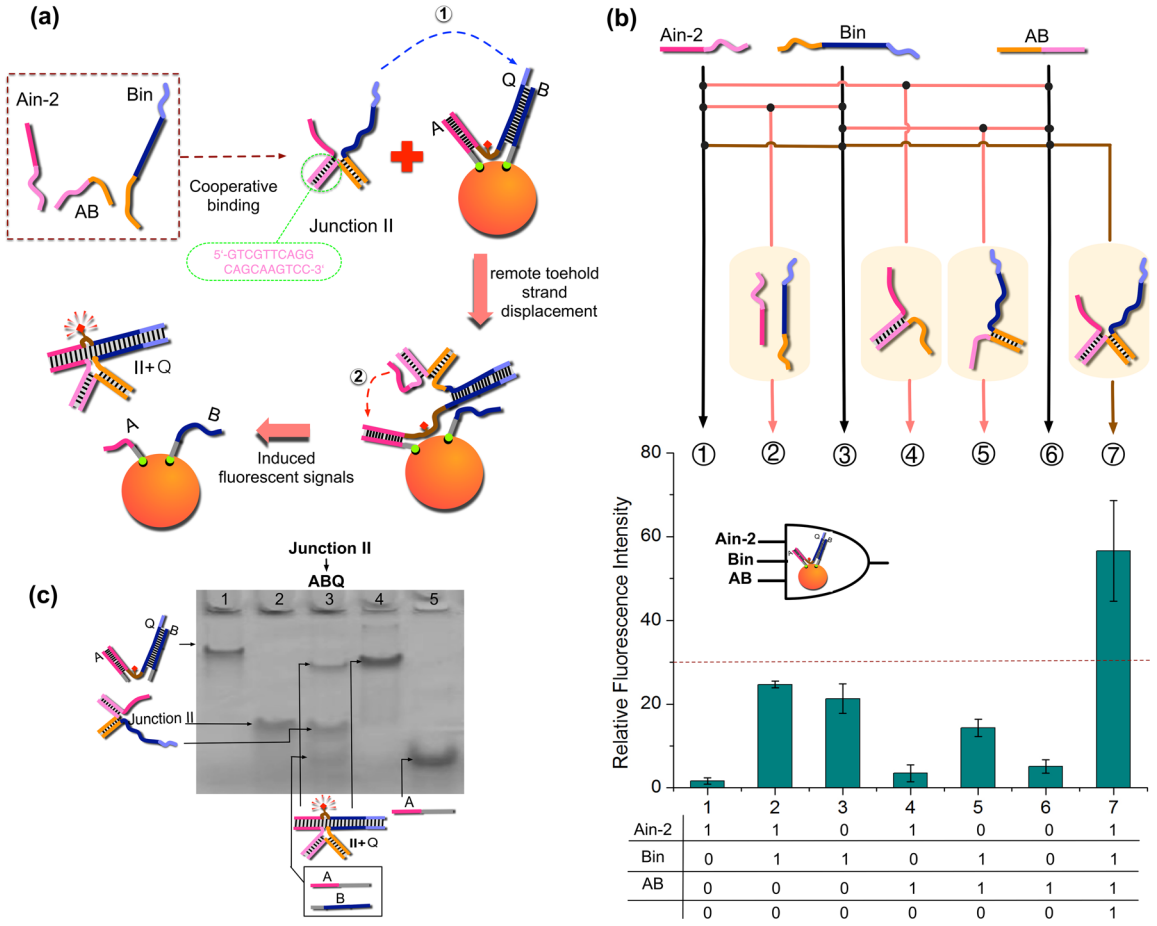

	①	②	③	④	⑤	⑥	⑦
Ain-2	1	1	0	1	0	0	1
Bin	0	1	1	0	1	0	1
AB	0	0	0	1	1	1	1
	0	0	0	0	0	0	1

Figure 3. Three-input "AND" logic gate G3. (a) Illustration of the design of the three-input "AND" gate. (b) Fluorescence results at 564 nm. Error bars represent one standard deviation from triplicate analysis. The threshold is set at half the highest signal value. (c) PAGE gel (12%) analysis of the gate. Lanes 1, 2, 4, and 5 correspond to different assembly polymers: ABQ, junction **II**, (**II+Q**), and strand A, respectively. Lane 3 corresponds to the computation results of the three-input logic gate after the addition of junction **II**.

As depicted in Figure 3a (step ①), with the help of the toehold, junction **II** can recognize strand Q via the toehold domain and then initiating the strand displacement reaction. Thus, this strand displacement can induce the separation of the fluorophore from the AuNP and greatly enhance the fluorescence intensity (Figure 3a, ②). Here, the computation was implemented by adding specific input strands to the gate solutions in seven ways (Figure 3b, ①–⑦). As expected, upon addition of only any one or two of the three inputs, no obvious fluorescence signal was detected, demonstrating that it was hard to trigger the strand displacement reaction with incomplete junction structures (Figure 3b, ①–⑥, lanes 1–6). However, when all three strands were present, junction **II** initiated remote strand displacement and induced the separation of the fluorophore from the AuNP, resulting in an enhanced fluorescence intensity (Figure 3b, ⑦, lane 7).

The PAGE results of the three-input gate are shown in Figure 3c. Similar to the two-input logic gate described above, only when all three input strands, Ain-2, Bin, and AB, were present was strand Q of gate G3 effectively displaced as shown in lane 3 (Figure 3c), resulting in the generation of the four-way junction structure **II+Q** byproduct. Other computing results were also obtained via gel analysis (Figure S3 of the Supporting Information).

Similarly, another three-input "AND" logic gate G4, with more structural complexity of binding assembling products, was implemented. As illustrated in Figure 4a, three separate strands, T1 (22 nucleotides), T2 (31 nucleotides), and T3 (24 nucleotides), would be cooperatively combined into junction **III** by binding recognition. After all three inputs were introduced, the displacement of strand Q was triggered. Accordingly, a great increase in fluorescence intensity was stimulated by the separation of the fluorophore from the AuNP (Figure 4a,b, ⑦, lane 7). However, upon addition of any one or two input strands, no significant fluorescence signals were detected (Figure 4b, ①–⑥, lanes 1–6). Interestingly, upon addition of inputs T1 and T2, a resultant fluorescence leakage was detected, which was a bit larger than those of other negative input combinations (Figure 4b, lane 2). The possible reason for this phenomenon is that the joint of T1 and T2 covers a major displacing region, which may partially serve as junction **III**. It is clear from these fluorescence data that logic gate G4 governed by junction **III** worked well as designed.

As displayed in Figure 4c, it is simple to see from PAGE gel results that no byproduct **III+Q** was generated when any two of the three inputs were introduced (Figure 4c, lanes 6, 8, and 9). In other words, strand Q was not displaced from structure ABQ. However, when junction **III** was cooperatively formed, structure **III+Q** was assembled as expected, and initial structure ABQ was dissembled accordingly (Figure 4c, lane 3). The PAGE results, consistent with the fluorescence results, demonstrated the proper execution of logic gate G4.

dx.doi.org/10.1021/am5036994 | ACS Appl. Mater. Interfaces 2014, 6, 14486–14492

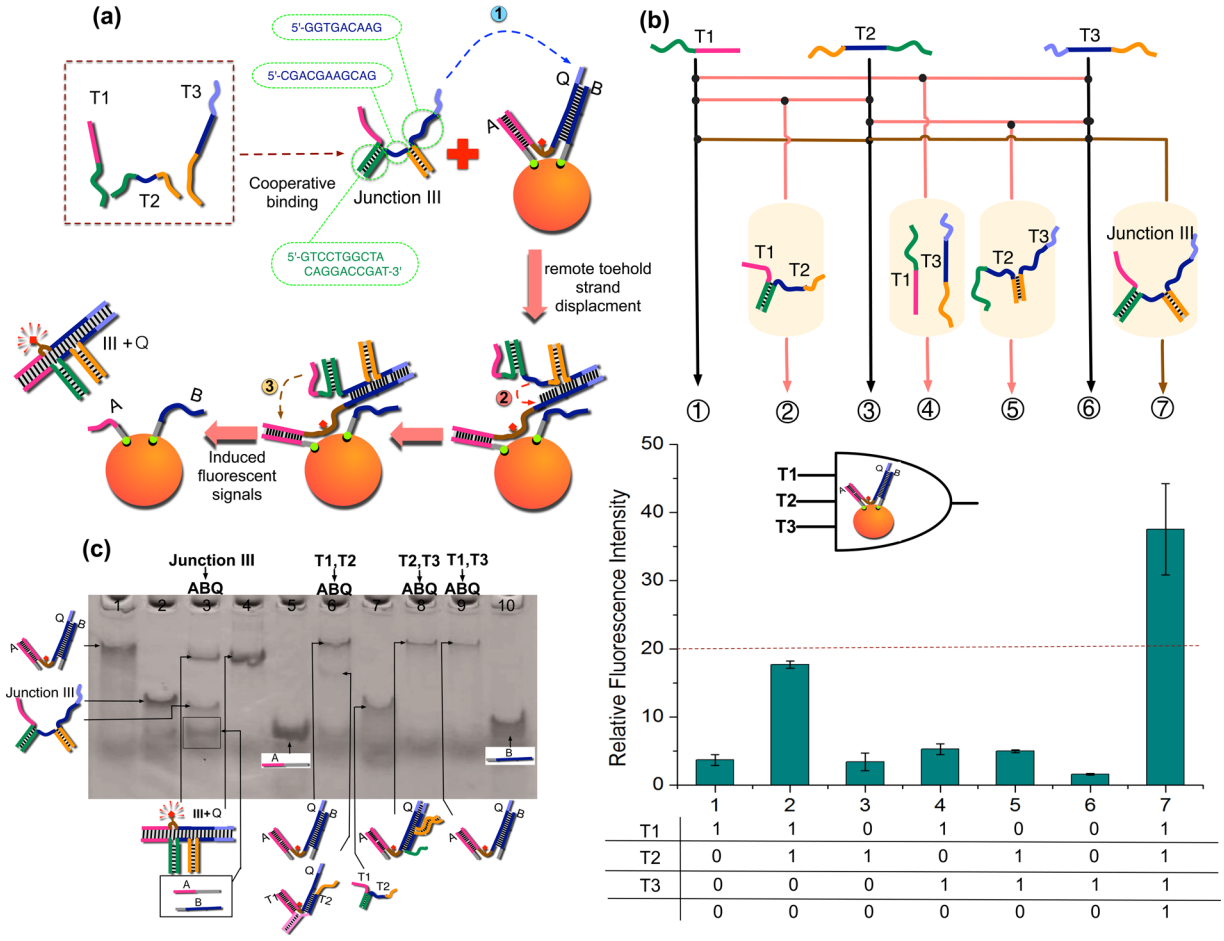

	1	2	3	4	5	6	7
T1	1	1	0	1	0	0	1
T2	0	1	1	0	1	0	1
T3	0	0	0	1	1	1	1
	0	0	0	0	0	0	1

Figure 4. Three-input "AND" logic gate G4. (a) Illustration of the design of the three-input "AND" gate. (b) Fluorescence results at 564 nm. The threshold is set at half the highest signal value. (c) PAGE gel (12%) analysis of the gate. Lanes 1, 2, 4, 5, 7, and 10 correspond to different assembly polymers: ABQ, junction **III**, (**III**+**Q**), strand A, T1/T2 complex, and strand B, respectively. Lanes 3, 6, 8, and 9 correspond to the computation results.

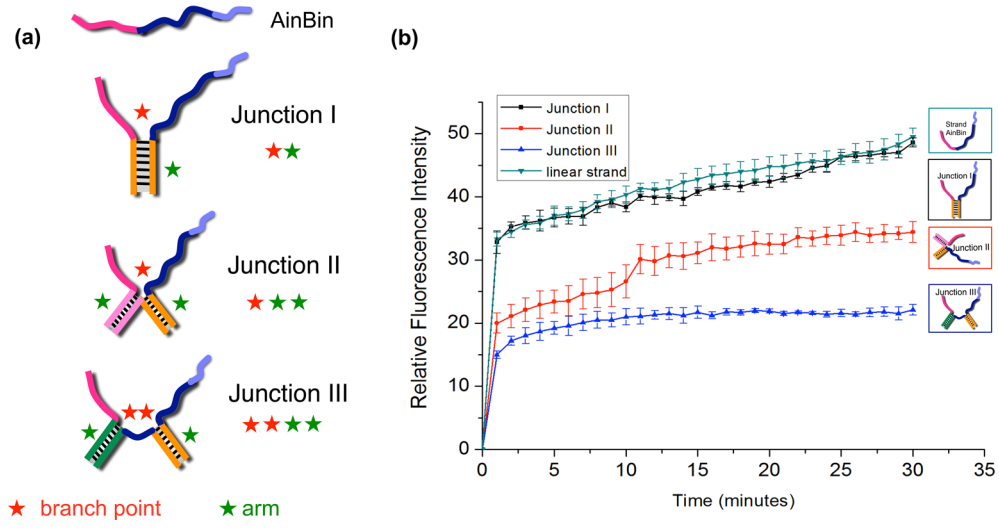

Figure 5. (a) Illustration of four different structures. Red stars represent branch points, and green stars represent protruding arms. (b) Comparison of kinetics induced by junctions **I**–**III**.

To test whether the complex junction structures of protruding arms and branch points did have an influence on the efficiency of the displacement reaction, the kinetics of strand displacement when using junctions **I**–**III** were compared by the relative released fluorescence intensity. Interestingly, with the increase in the structural complexity of the protruding arms, the increments of fluorescent intensity were inhibited accordingly (Figure 5). As demonstrated in Figure 4, after a 30 min reaction, the detected fluorescence intensity induced by junction **I** showed an increment of 48.6%, which was very close to the increment of

dx.doi.org/10.1021/am5036994 | *ACS Appl. Mater. Interfaces* 2014, 6, 14486–14492

49.5% when using linear input strand AinBin. Likewise, junction **II** showed a fluorescence increment of 34.4%, smaller than that of junction **I**. The most complicated structures, junction **III**, had the lowest fluorescence increment of 22.1%. The reason may be that junction **I** has only one protruding arm and branch point, whose structure is most similar to that of linear strand AinBin. Therefore, the displacing ability of junction **I** is substantially equal to that of strand AinBin. In contrast, with the more complicated junction structures, junctions **II** and **III** have difficulty implementing remote toehold strand displacement, leading to a rather smaller fluorescence increment.

Additionally, we further utilized the assembly DNA/AuNPs conjugates to implement two-input gate G5. In this experiment, Q-sh, modified with a thiol group at the 5′ end, was attached to 5 nm AuNPs, forming conjugate C1. On the other hand, strands A and B were attached to 15 nm AuNPs to yield conjugate C2. Then, conjugate C1 was hybridized with conjugate C2 to produce an AuNP dimer (5 + 10 nm) as the initial structures (Figure 6a,b). Upon addition of inputs Ain and Bin (forming junction **I**), the dimers were dismembered, because 5 nm conjugate C1 could be displaced by junction **I** and separated with 10 nm conjugate C2. As a result, a number of 5 and 10 nm AuNP pairs were difficult to observe in TEM images, thus demonstrating a successful operation of two-input gate G5 (Figure 6b and Figure S6 of the Supporting Information). In the statistical results, before strand displacement, 102 conjugates are counted, and the rate of generation of particle dimers is 84.3% (Figure 6c). Interestingly, upon addition of inputs Ain and Bin, 80 separated conjugates are counted, and the percentage of dissociated particles is 88.8% (Figure 6c).

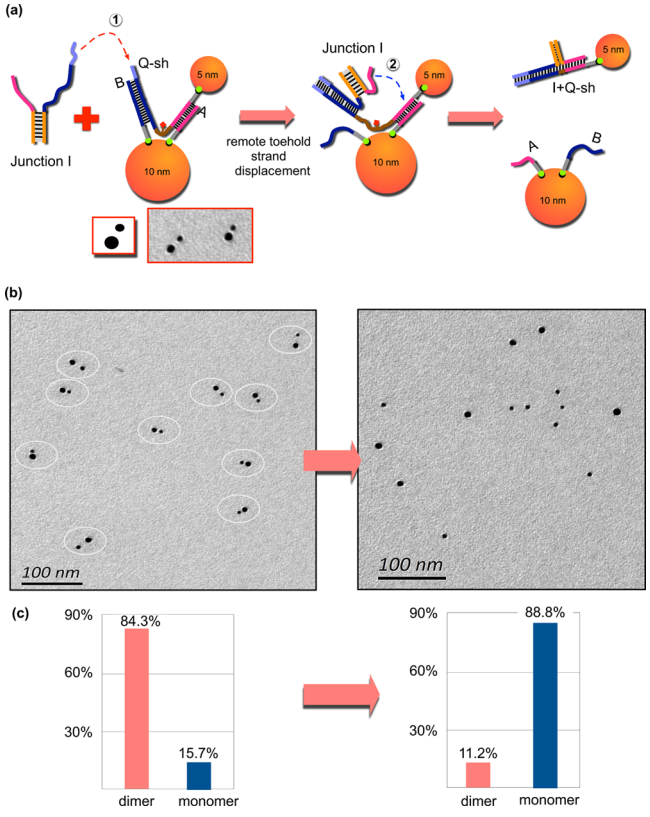

Figure 6. (a) Illustration of two-input gate G5 using the assembly DNA/AuNPs conjugates. (b) AuNP conjugates visualized by TEM. The scale bar is 100 nm. (c) Statistical results of TEM images.

CONCLUSION

In conclusion, a logic computing system is constructed via the binding-induced mechanism, using the AuNP-based beacons, in which five multiple-input logic gates have been implemented. Importantly, a remote strand displacement reaction can be triggered by a binding-induced method, in which multiple DNA inputs cooperatively recognize each other. Furthermore, the system can recognize DNA and protein SA simultaneously. Interestingly, it is observed that, with the increase in the structural complexity of the combinational DNA inputs, the increments of fluorescence intensity can be significantly inhibited. Finally, the manipulations of the multiple-input logic system are also demonstrated by controlling programmed conjugate DNA/AuNP clusters. This mechanism not only provides possibilities for the detection, design, and manipulation of complex nanodevices but also can be widely applied in the detection of multiple molecular targets and the construction of a large-scale DNA-based computation.

ASSOCIATED CONTENT

Supporting Information

Materials, experimental methods, and additional experimental data. This material is available free of charge via the Internet at http://pubs.acs.org.

AUTHOR INFORMATION

Corresponding Authors

*E-mail: yangjing369@gmail.com.
*E-mail: zhangcheng369@pku.edu.cn.
*E-mail: lqpan@mail.hust.edu.cn.

Author Contributions

J.Y. and C.D. contributed equally to this work.

Notes

The authors declare no competing financial interest.

ACKNOWLEDGMENTS

We thank Prof. H. Inaki Schlaberg for helpful discussion and manuscript revision. This research is supported by the National Natural Science Foundation of China (Grants 61370099, 61272161, 61127005, 61133010, 61272246, 61033003, and 61320106005), the Beijing Excellent Talent Training Project (2013D009005000002), the Programme of Introducing Talents of Discipline to Universities (B13009), and Fundamental Research Funds for the Central University (13QN14).

ABBREVIATIONS

SA = streptavidin
TEM = transmission electron microscopy
PAGE = native polyacrylamide gel electrophoresis

REFERENCES

(1) Mao, C. D.; LaBean, T. H.; Reif, J. H.; Seeman, N. C. Logical Computation Using Algorithmic Self-assembly of DNA Triple-cross-over Molecules. *Nature* **2000**, *407*, 493−496.
(2) Seelig, G.; Soloveichik, D.; Zhang, D. Y.; Winfree, E. Enzyme-free Nucleic Acid Logic Circuits. *Science* **2006**, *314*, 1585−1588.
(3) Li, W.; Yang, Y.; Yan, H.; Liu, Y. Three-Input Majority Logic Gate and Multiple Input Logic Circuit based on DNA Strand Displacement. *Nano Lett.* **2013**, *13*, 2980−2988.
(4) Qian, L.; Winfree, E. Scaling Up Digital Circuit Computation with DNA Strand Displacement Cascades. *Science* **2011**, *332*, 1196−1201.

(5) Pei, H.; Liang, L.; Yao, G.; Li, J.; Huang, Q.; Fan, C. Reconfigurable Three-Dimensional DNA Nanostructures for the Construction of Intracellular Logic Sensors. *Angew. Chem., Int. Ed.* **2012**, *51*, 9020−9024.
(6) Rinaudo, K.; Bleris, L.; Maddamsetti, R.; Subramanian, S.; Weiss, R.; Benenson, Y. A Universal RNAi-based Logic Evaluator That Operates in Mammalian Cells. *Nat. Biotechnol.* **2007**, *25*, 795−801.
(7) Picuri, J. M.; Frezza, B. M.; Ghadiri, M. R. Universal Translators for Nucleic Acid Diagnosis. *J. Am. Chem. Soc.* **2009**, *131*, 9368−9377.
(8) Xia, F.; Zuo, X.; Yang, R.; White, R. J.; Xiao, Y.; Kang, D.; Gong, X.; Lubin, A. A.; Vallée, B. A.; Yuen, J. D.; Hsu, B. Y.; Plaxco, K. W. Label-Free, Dual-Analyte Electrochemical Biosensors: A New Class of Molecular-Electronic Logic Gates. *J. Am. Chem. Soc.* **2010**, *132*, 8557−8559.
(9) Pei, H.; Zuo, X.; Zhu, D.; Huang, Q.; Fan, C. Functional DNA Nanostructures for Theranostic Applications. *Acc. Chem. Res.* **2014**, *47*, 550−559.
(10) Stojanovic, M. N.; Stefanovic, D. A Deoxyribozyme-based Molecular Automaton. *Nat. Biotechnol.* **2003**, *21*, 1069−1074.
(11) Elbaz, J.; Lioubashevski, O.; Wang, F.; Remacle, F.; Levine, R. D.; Willner, I. DNA Computing Circuits Using Libraries of DNAzyme Subunits. *Nanotechnology* **2010**, *5*, 417−422.
(12) Zhu, J.; Li, T.; Zhang, L.; Dong, S.; Wang, E. G-quadruplex DNAzyme based Molecular Catalytic Beacon for Label-free Colorimetric Logic Gates. *Biomaterials* **2011**, *32*, 7318−7324.
(13) Zhu, J.; Yang, X.; Zhang, L.; Zhang, L.; Zhang, L.; Lou, B.; Dong, S.; Wang, E. A Visible Multi-digit DNA Keypad Lock Based on Split G-quadruplex DNAzyme and Silver Microspheres. *Chem. Commun.* **2013**, *49*, 5459−5461.
(14) Liu, X.; Aizen, R.; Freeman, R.; Yehezkeli, O.; Willner, I. Multiplexed Aptasensors and Amplified DNA Sensors Using Functionalized Graphene Oxide: Application for Logic Gate Operations. *ACS Nano* **2012**, *6*, 3553−3563.
(15) Song, S.; Liang, Z.; Zhang, L.; Wang, L.; Li, G.; Fan, C. Gold-Nanoparticle-based Multicolor Nanobeacons for Sequence-Specific DNA Analysis. *Angew. Chem., Int. Ed.* **2009**, *48*, 8670−8674.
(16) Jiang, Q.; Wang, Z.; Ding, B. Programmed Colorimetric Logic Devices based on DNA−Gold Nanoparticle Interactions. *Small* **2013**, *9*, 1016−1020.
(17) Zhang, J.; Song, S.; Wang, L.; Pan, D.; Fan, C. A Gold Nanoparticle-based Chronocoulometric DNA Sensor for Amplified Detection of DNA. *Nat. Protoc.* **2007**, *2*, 2888−2895.
(18) Pei, H.; Li, F.; Wan, Y.; Wei, M.; Liu, H.; Su, Y.; Chen, N.; Huang, Q.; Fan, C. Designed Diblock Oligonuclueotide for the Synthesis of Spatially Isolated and Highly Hybridizable Functionalization of DNA-Gold Nanoparticle Nanoconjugates. *J. Am. Chem. Soc.* **2012**, *134*, 11876−11879.
(19) Shukoor, M. I.; Altman, M. O.; Han, D.; Bayrac, T. A.; Ocsoy, I.; Zhu, Z.; Tan, W. Aptamer-Nanoparticle Assembly for Logic-based Detection. *ACS Appl. Mater. Interfaces* **2012**, *4*, 3007−3011.
(20) Zhang, L.; Zhang, Y.; Liang, R.; Qiu, J. Colorimetric Logic Gates Based on Ion-dependent DNAzymes. *J. Phys. Chem. C* **2013**, *117*, 12352−12357.
(21) Qian, L.; Winfree, E.; Bruck, J. Neural Network Computation with DNA Strand Displacement Cascades. *Nature* **2011**, *475*, 368−372.
(22) Elbaz, J.; Lioubashevski, O.; Wang, F.; Remacle, F.; Levine, R. D.; Willner, I. DNA Computing Circuits Using Libraries of DNAzyme Subunits. *Nat. Nanotechnol.* **2010**, *5*, 417−422.
(23) Frezza, B. M.; Cockroft, S. L.; Ghadiri, M. R. Modular Multi-level Circuits from Immobilized DNA-based Logic Gates. *J. Am. Chem. Soc.* **2007**, *129*, 14875−14879.
(24) Yurke, B.; Turberfield, A. J.; Mills, A. P., Jr.; Simmel, F. C.; Neumann, J. L. A DNA-fuelled Molecular Machine Made of DNA. *Nature* **2000**, *406*, 605−608.
(25) Yin, P.; Choi, H. M. T.; Calvert, C. R.; Pierce, N. A. Programming Biomolecular Self-assembly Pathways. *Nature* **2008**, *451*, 318−322.
(26) Zhang, C.; Wu, L.; Yang, J.; Liu, S.; Xu, J. A Molecular Logical Switching Beacon Controlled by Thiolated DNA Signals. *Chem. Commun.* **2013**, *49*, 11308−11310.
(27) Chen, X. Expanding the Rule Set of DNA Circuitry with Associative Toehold Activation. *J. Am. Chem. Soc.* **2012**, *134*, 263−271.
(28) Zhu, J.; Zhang, L.; Dong, S.; Wang, E. Four-Way Junction-Driven DNA Strand Displacement and Its Application in Building Majority Logic Circuit. *ACS Nano* **2013**, *7*, 10211−10217.
(29) Das, P. C.; Puri, A. Energy Flow and Fluorescence near a Small Metal Particle. *Phys. Rev. B* **2002**, *65*, 155416−155418.
(30) Dulkeith, E.; Morteani, A. C.; Niedereichholz, T.; Klar, T. A.; Feldmann, J.; Levi, S. A.; van Veggel, F.; Reinhoudt, D. N.; Möller, M.; Gittins, D. I. Fluorescence Quenching of Dye Molecules near Gold Nanoparticles: Radiative and Nonradiative Effects. *Phys. Rev. Lett.* **2002**, *89*, 203002−203005.
(31) Zhang, J.; Wang, L.; Zhang, H.; Boey, F.; Song, S.; Fan, C. Aptamer-based Multicolor Fluorescent Gold Nanoprobes for Multiplex Detection in Homogeneous Solution. *Small* **2009**, *6*, 201−204.
(32) Wang, J.; Liu, G.; Merkoci, A. Electrochemical Coding Technology for Simultaneous Detection of Multiple DNA Targets. *J. Am. Chem. Soc.* **2003**, *125*, 3214−3215.
(33) Oh, E.; Hong, M. Y.; Lee, D.; Nam, S. H.; Yoon, H. C.; Kim, H. S. Inhibition Assay of Biomolecules based on Fluorescence Resonance Energy Transfer (FRET) between Quantum Dots and Gold Nanoparticles. *J. Am. Chem. Soc.* **2005**, *127*, 3270−3271.
(34) Yang, J.; Shen, L.; Ma, J.; Schlaberg, H. I.; Liu, S.; Xu, J.; Zhang, C. Fluorescent Nanoparticle Beacon for Logic Gate Operation Regulated by Strand Displacement. *ACS Appl. Mater. Interfaces* **2013**, *5*, 5392−5396.
(35) Genot, A. J.; Zhang, D. Y.; Bath, J.; Turberfield, A. J. Remote Toehold: A Mechanism for Flexible Control of DNA Hybridization Kinetics. *J. Am. Chem. Soc.* **2011**, *133*, 2177−2182.